High density resolution in synchrotron-radiation-based attenuation-contrast microtomography

Felix Beckmann, Julia Herzen, Astrid Haibel, Bert Müller[a], and Andreas Schreyer

Institute for Materials Research, GKSS Research Center, Geesthacht, Germany;
[a]Biomaterials Science Center (BMC), University of Basel, Basel, Switzerland

ABSTRACT

During the last few years microtomography using synchrotron radiation (SR) has become a standard technique to characterize samples 3-dimensionally in the fields of biology, medicine and materials science. The GKSS Research Center Geesthacht, Germany, is responsible for developing and running the microtomography experiments at the SR-facility DESY, Hamburg, Germany. The application of SRμCT using attenuation-contrast at the beamlines W2/HARWI-II and BW2 of the storage ring DORIS III results in high throughput investigations. For achieving tomograms showing not only high spatial resolution but also high density resolution special emphasis was given to the stability of the used monochromators and the calibration of the total system. The influence of the photon statistics from the measurement to the tomograms is simulated and the achieved density resolution is demonstrated showing selected results.

Keywords: attenuation contrast, density resolution, synchrotron radiation, tomography, microtomography, spatial resolution

1. INTRODUCTION

Over approximately the last 10 years X-ray microtomography using synchrotron radiation (SRμCT) at the Deutsches Elektronen-Synchrotron DESY has evolved as an increasingly accepted and utilized technique for characterizing the 3D internal structure of samples in the fields of materials science, biological and medical applications.[1–3] This development is supported by the increasing spatial resolution and density resolution of the 3D images, which can now be routinely obtained in the micrometer range. In 2002 the GKSS-Research center became responsible for the operation of the microtomography experiment at DESY. The GKSS HARWI-II wiggler beamline at DORIS III is now in routine operation providing a large beam with a cross section in the range of square centimeters for the investigation of large objects in the photon energy range from 20 to 250 keV.[4,5] The low photon energy range (8 to 24 keV) is covered by the wiggler beamline BW2 at DORIS III. Furthermore, at the PETRA III storage ring two undulator beamlines with imaging capability are currently constructed by GKSS. The imaging beamline (IBL) will provide a nanotomography as well as a microtomography station for X-ray energies up to 50 keV. The High Energy Materials Science beamline HEMS will, apart from various diffraction setups, also offer a microtomography experiment optimized for X-ray energies starting from 30 keV. The concept and features of these beamlines are described in a different paper in this proceeding.[6]

The insertion devices BW2 and HARWI-II at the second generation synchrotron radiation source DORIS III provide for a large, high flux, and incoherent X-ray beam. By sophisticated double crystal fixed exit monochromators an optimized X-ray source is used for performing pure attenuation-contrast microtomography. The high photon statistics in the monochromtatized X-ray beam, together with the carefully calibration of the microtomgraphy device allows for tomograms showing not only high spatial, but also high density resolution. In the following chapter the influence of the statistics achieved in the X-ray detector to the density resolution is discussed following the concept previously developed.[7] The different features of the tomography experiment at the beamlines BW2 and HARWI-II will be given and the shown results will demonstrate the achieved high spatial and high density resolution which were achieved in standard user experiments for different types of samples.

Further author information: (Send correspondence to F.B.)
F.B: E-mail: felix.beckmann@gkss.de, Telephone: +49 40 8998 5309

Developments in X-Ray Tomography VI, edited by Stuart R. Stock,
Proc. of SPIE Vol. 7078, 70781D, (2008) · 0277-786X/08/$18 · doi: 10.1117/12.794617

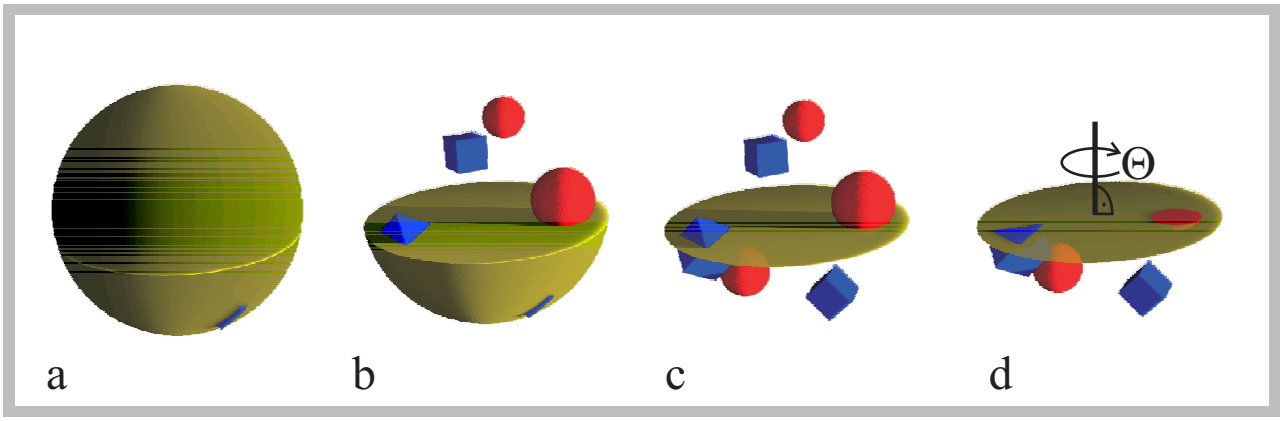

Figure 1. Volume renderings of the virtual sample used for simulations. The used components are defined in table 1. a: Total view of the sample. b,c,d: Virtual cut of the *embedding* material showing the slice perpendicular to the rotation axis, which is shown as a typical slice in figs. 1d, 2 and 3.

2. SIMULATION

To study the influence of photon statistics the measurement process is simulated using the software IDL, ITT Visual Information Solutions, Boulder, USA. As the synchrotron radiation source allows for an intense monochromatic X-ray beam with low divergence, parallel beam tomography for a defined photon energy is simulated.

2.1 Parallel beam tomography

For the simulation we defined a virtual 3D object consisting of several spheres and cubes. The basic volume of the sample consists of 501 x 501 x 501 voxels. The sample is defined by the combination of the objects presented in table 1. The position is given in percentage of the maximal size of 501. Furthermore, two boxes are tilted in the volume. In figure 1 volume renderings of the defined sample are given. The shown slice in figure 1d is perpendicular to the rotation axis and used in the following to demonstrate the influence of the statistics to the density resolution. The concept of 3D imaging using parallel-beam geometry is based on recording a set of 2D projections of the specimen at different sample rotations. For simulation we use a detector size of 501 x 501 pixels. The maximum projected attenuation of the sample is about 2. For the shown simulated measurement projections were calculated from 0 to 180° with an angular increment of 0.5°. In figure 2 the measurement process is demonstrated. Three different projections are given in figure 2a. For three different heights (I, II, III) the corresponding sinograms are presented in figure 2b. A single line in the sinogram is calculated by the Radon transform of the corresponding slice which is perpendicular to the rotation axis of the sample (s. figs. 2c and 1d).

Table 1. Composition of the virtual sample. Several spheres and cubes are used for the simulation. The attenuation values are manually choosen to obtain a maximal projected attenuation of 2. The size of x,y,z, and radius are given in percent.

SHAPE	X	Y	Z	RADIUS	ATTENUATION	COLOR
sphere	45	42	50	40	0.002595	Yellow
sphere	20	45	50	10	0.006986	Red
sphere	60	40	25	11.8	0.006986	Red
sphere	40	50	75	6.67	0.006986	Red
cube	65	22	40	12.5	0.009980	Blue
cube	58	62	60	11.1	0.009980	Blue
cube	26	26	37	10	0.009980	Blue

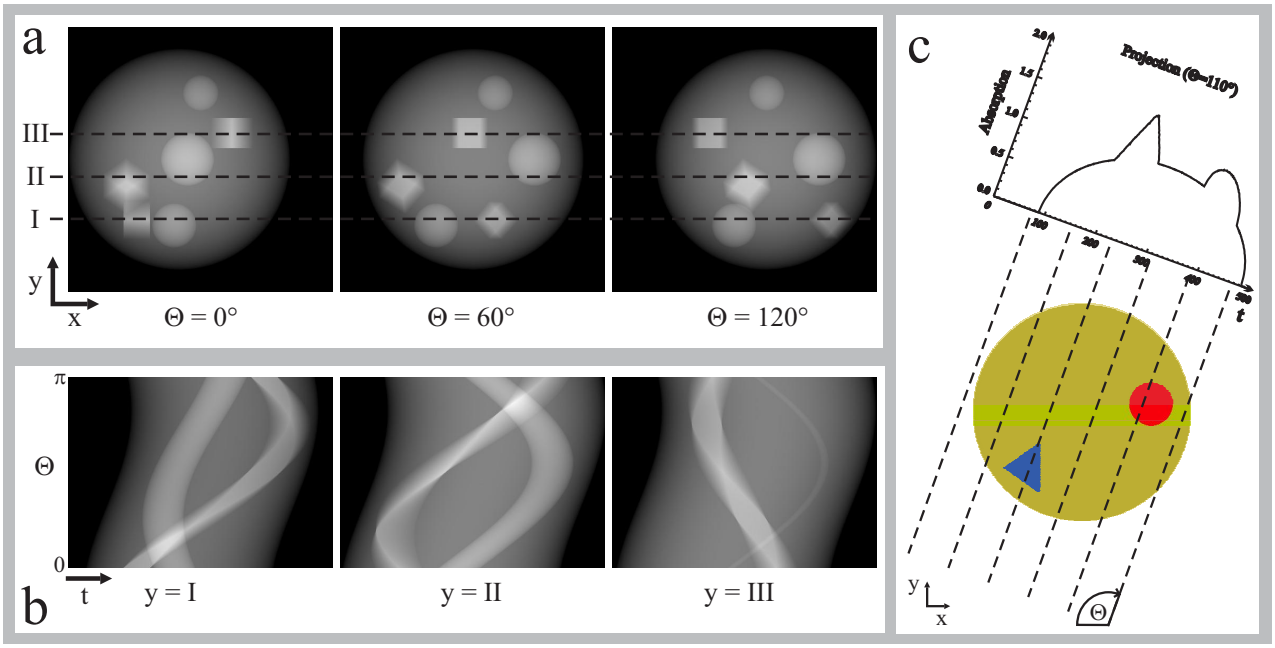

Figure 2. Demonstration of the measurement process for parallel beam tomography. a: Attenuation projection for different sample rotation. b: Sinograms for different heights I, II, III shown in a. c: Radon transform for one rotation of a single slice.

Assuming the implementation of optimal measurement conditions, which should, therefore, result in an artifact free reconstruction, the simulation of a standard tomographic measurement and reconstruction was performed for detector systems which differ in the number of distinguishable analog digital units (ADU). For each projection an image with sample and without sample is calculated. Noise using the random generator for Poisson statistics in IDL is added to the images. The reconstruction is then performed following the standard reconstruction queue used for SRμCT at DESY.

2.2 Density resolution

For SRμCT, where optimal source and beam geometry is used, the quality of the obtained microtomography data is given by the spatial resolution and the density resolution of the system. The spatial resolution can be measured by obtaining the modulation transfer function (MTF). The density resolution is given by the ability to detect different attenuations in the tomogram.

For different ADUs characteristics of the detector a resulting single reconstructed slice, the histogram of all slices and the obtained Gauss fits to the histogram are given in figure 3. The ADUs are selected to realize the optimal detector (fig. 3a), an detector using slow speed digitization at 16bit (fig. 3b), medium speed at 14bit (fig. 3c) and high speed at 11bit (fig. 3d). The given digitization depths are standardly available for different CCD systems of several companies.

It can clearly be seen that for low-statistical qualities of the used detector the different absorbing materials can hardly be separated. It has to be mentioned that the results are only valid for an undisturbed measurement. For X-ray sources having a very large bandwidth or fast varying beam profiles systematic errors will be introduced to the tomograms and an automatic segmentation of different materials in the volume will become very difficult or even impossible. Furthermore, for very high spatial resolution in the tomogram the required mechanical stability for sample manipulation and repositioning is very important. Therefore, to specify the density resolution of a microtomography experiment at a synchrotron radiation facility the entire system has to taken into account.

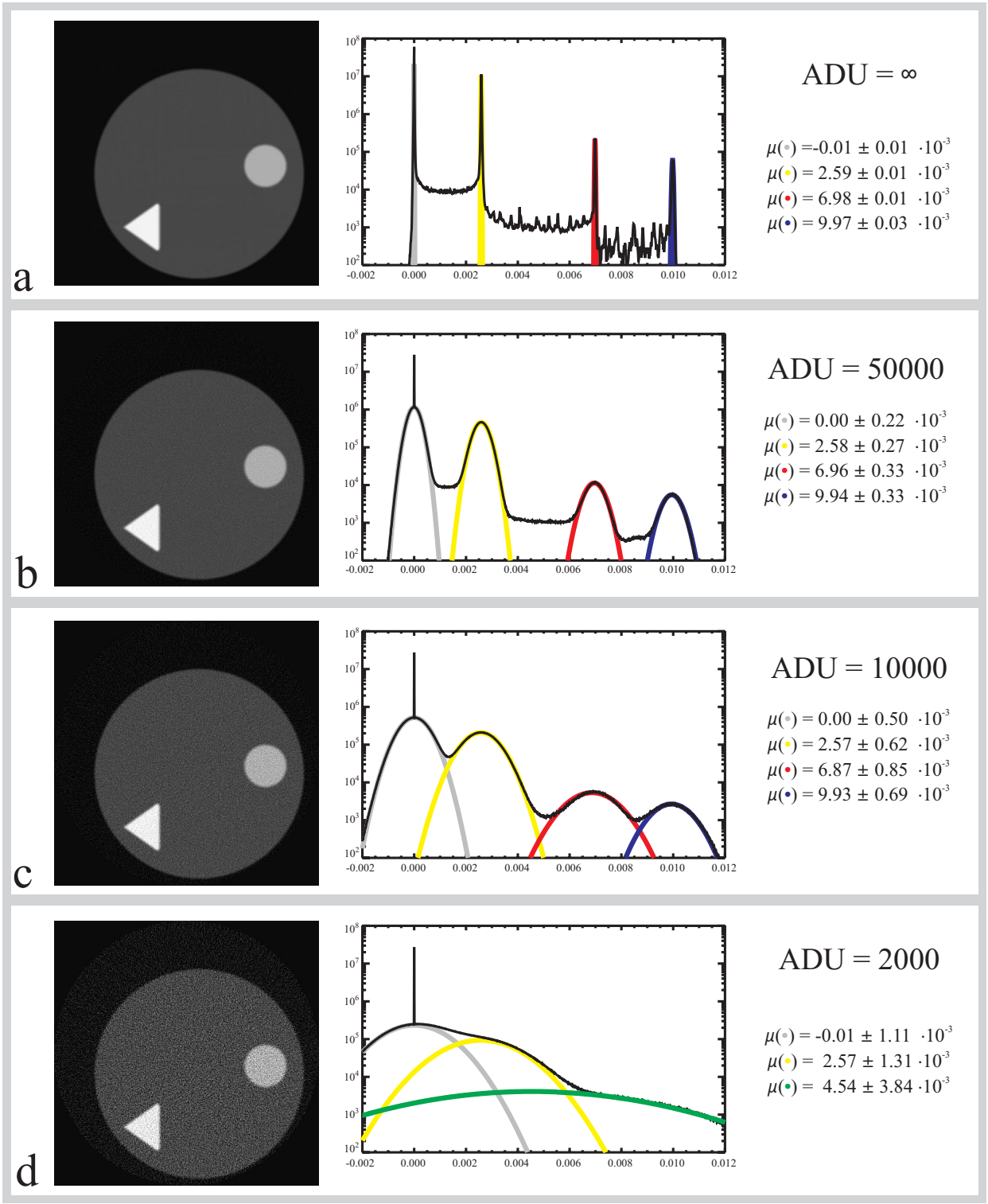

Figure 3. Reconstruction of the simulated measurement of the sample shown in figs. 1, 2, defined in table 1. Left: reconstructed slice; Middle: histogram of all slices representing the frequency of different attenuation values. Right: parameters of fitted Gauss peaks. The detector quality, represented by the amount of distinguishable ADUs, is decreasing from a) to d) resulting in a low density resolution in d) where the spheres and cubes cannot be distinguished in the histogram.

3. EXPERIMENT

Microtomography at DORIS III is in the tenth year of user operation. The basic developments of the tomographical system were performed at the wiggler beamline BW2 using low photon energies from 8 to 24 keV. For higher photon energies starting at 20 keV the apparatus can be temporarily installed at the high energy materials science beamline W2 at the wiggler HARWI-II. The dedicated setup for performing high-energy SRμCT for large and small samples at beamline W2/HARWI-II is currently under construction and will be available mid of 2009. Furthermore, at the storage ring PETRA III micro- and nanotomography for small specimen will become available starting end of 2009. Here we concentrate on the instrumentation and features of the SRμCT at DORIS III.

3.1 Storage ring DORIS III

The second-generation synchrotron radiation facility DORIS III provides for a large and intense X-ray source. Positrons are stored at an energy of about 4.5 GeV, a current of about 150 mA, and a life time of 15 h. Normally every 8 hours the positrons will be refilled. The different available experimental stations are shown in figure 4a.

Low-energy beamline BW2

The insertion device BW2 is optimized for producing photon energies up to 24 keV. A double crystal fixed-exit monochromator (Si(111)-crystals) allows for selecting photon energies in the range of about 8 to 24 keV.[8,9] Below 11 keV two Au-coated mirrors can be added to reduced the thermal load on the monochromator. For performing microtomography special emphasize is given to optimize the beam profile. Depending on the heat load on the first crystal of the monochromator the first crystal is bend to produce a large monochromatic photon beam (width 15 mm, height 3.5 mm). Three different modes are currently foreseen for the different photon energies:

	BW2	**BW2**	**BW2**
wiggler gap	40 mm	40 mm	50 mm
mirrors (Au coated):	without	with	without
photon energy:	14-24 keV	8-11 keV	8 - 14 keV
sample height:	3.5 mm	1.5 mm	2.5 mm
sample width:	10 mm	10 mm	10 mm

High-energy beamline HARWI-II/W2

In autumn 2005 the GKSS-Research Center in cooperation with DESY, Hamburg, started operation of the synchrotron radiation beamline HARWI-II. The beamline is specialized for materials science experiments using hard X-rays. It has been in routine user operation since 2006. The photon flux of the HARWI-II wiggler is shown in figure 4b. By use of different filters the photon spectrum can be modified to reduce the heat load on the first monochromator crystal. Two monochromators are installed. One is optimized for diffraction experiments and the other is optimized for imaging applications. The fixed-exit monochromator for imaging applications consists of different sets of crystals and allows using an intense and large monochromatic X-ray beam in the energy range of 20 to 200 keV. A detailed description of the monochromator is given elsewhere.[4] The combinations of filters and crystals is selected according to the dedicated photon energy:

	HARWI-II/W2	**HARWI-II/W2**	**HARWI-II/W2**	**HARWI-II/W2**
photon energy:	20-30 keV	30-60 keV	60-200 keV	60-200 keV
filter:	3 mm C	10 mm C	10 mm C + 1 mm Cu	10 mm C + 2 mm Cu
sample height:	4 mm	5 mm	7 mm	7 mm
sample width:	70 mm	70 mm	10 mm	70 mm

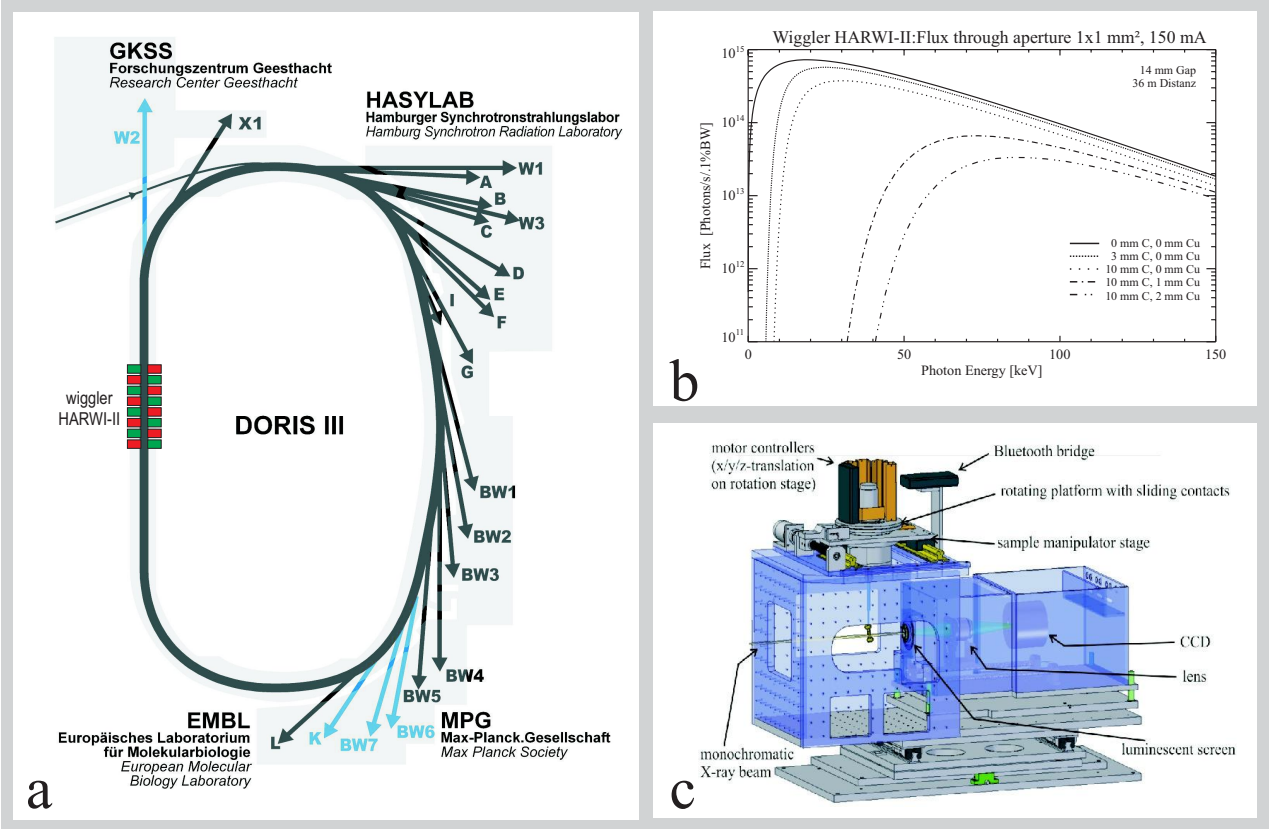

Figure 4. Microtomography at DORIS III: a: Experimental stations at DORIS III. Microtomography is performed at beamlines BW2 and HARWI-II/W2. The insertion device for beamline W2 is the wiggler HARWI-II. b: Photon spectrum of the HARWI-II wiggler for different sets of filters. c: Experimental setup used for microtomography at beamlines BW2 and HARWI-II/W2.

3.2 experimental setup and SRμCT measurement

The schematic setup used for absorption-contrast microtomography is presented in figure 4c. It consists of a 2D X-ray detector and a sample manipulator stage. The sample manipulator provides both the rotation and the lateral positioning of the specimen. The incident X-rays are converted into visible light which then is projected onto a CCD camera by an optical lens system. The used components are:

CCD camera:	KX2, Apogee Instruments, Inc.; 14 bit digitalization at 1.25 MHz, $1536 \cdot 1024$ pixel^2; each $9 \cdot 9$ μm^2
optical lens:	camera lens, Nikon Inc., 35 mm or 50 mm focal length
fluorescent screen:	$CdWO_4$ single crystal, thickness 200μm - 1000μm

The sample manipulator is designed to allow for continuous rotation. CANBUS motor electronics (CAN-STEPCON-1H of ESD Electronics, Hannover, Germany) was installed onto the rotation platform. The power supply is provided by sliding contacts and the signals for motor control are transferred by a Bluetooth bridge (CAN-BLUETOOTH, ESD Electronics, Hannover, Germany).

For absorption-contrast microtomography typically a set of 720 radiograms at different sample rotations equally stepped between 0 and π were taken. The tomographical reconstructions were calculated by using backprojection of filtered projection.[10] For this reconstruction method the center of rotation is determined within a fraction of pixel by an automatized algorithm.[11]

High-density resolution in standard user mode

The microtomography system operated by the GKSS at DESY is designed to perform SRμCT investigations in user mode. The alignment and optimization of the beamline and the apparatus is done by the GKSS. The preparation of the sample and the on-site controlling of the measurement is done by the different user groups. The data management for optimized reconstruction is operated by the GKSS.

For providing a robust measurement system with optimized, objective and reproducable performance several features are adjusted for each measurement:

Photon energy:	The optics of the beamline is optimized to provide for a monochromatic, stable X-ray beam. The photon energy is selected to optimize the contrast in the sample. For homogeneous samples an maximal projected attenuation of about 2 is selected.[12]
Optical magnification:	The field of view of the used X-ray detector is matched to the size of the sample. The apparatus allows for continuous variation of the optical magnification (s. figure 4c).
Spatial resolution:	For each selected photon energy and optical magnification the MTF of the total system is determined by measuring the projection of an edge material - gold for low photon energy and DENSIMED for high photon energies.[13]
Density resolution:	The exposure time of the system is altered during the scan to always use the full detector statistics.
Multiple scans:	For samples which are larger than the field of view of the detector different scanning techniques are integrated. If the width of the sample is larger, the rotation axis of the system is shifted and several scans are performed. Before reconstruction the projections are combined to build one tomographical scan.[14] If the height of the sample is larger than the height of the field of view of the detector, several scans are performed with the sample shifted vertically. After tomographic reconstruction the different volumes are combined to build one reconstructed volume.[15]
Increasing density resolution:	To be able to enhance the density resolution of the total system the number of images taken with and without sample can be increased. Another option is to choose a smaller field of view of the X-ray detector and apply scanning techniques. This allows for an increase of the exposure time and therefore for a higher photon statistics. This technique is now routinely used for increasing the photon statistics if required.

For reconstruction an queue is implemented which semi automatically operate the data flow. The installed computer hardware, including data backup, can treat the data throughput of the present tomography system. Therefore, for the standardized scans, including the scanning option mentioned above, the reconstructed data is available in the range of the scan time after the scan. The user can optimize the density resolution with respect to the spatial resolution in the tomogram by using binning of the raw measured data.[16] For special needs several reconstruction with different binning values for the raw data are performed. The reconstructed data format can be choosen by the user. Measurement and reconstructed data are normally copied to external hard disks and transferred to the user's facilities. Furthermore, 3D data sets are created, which can be processed with the software MyVgi, Volume Graphics GmbH, Heidelberg, Germany, to provide for a first glance on the reconstructed data.

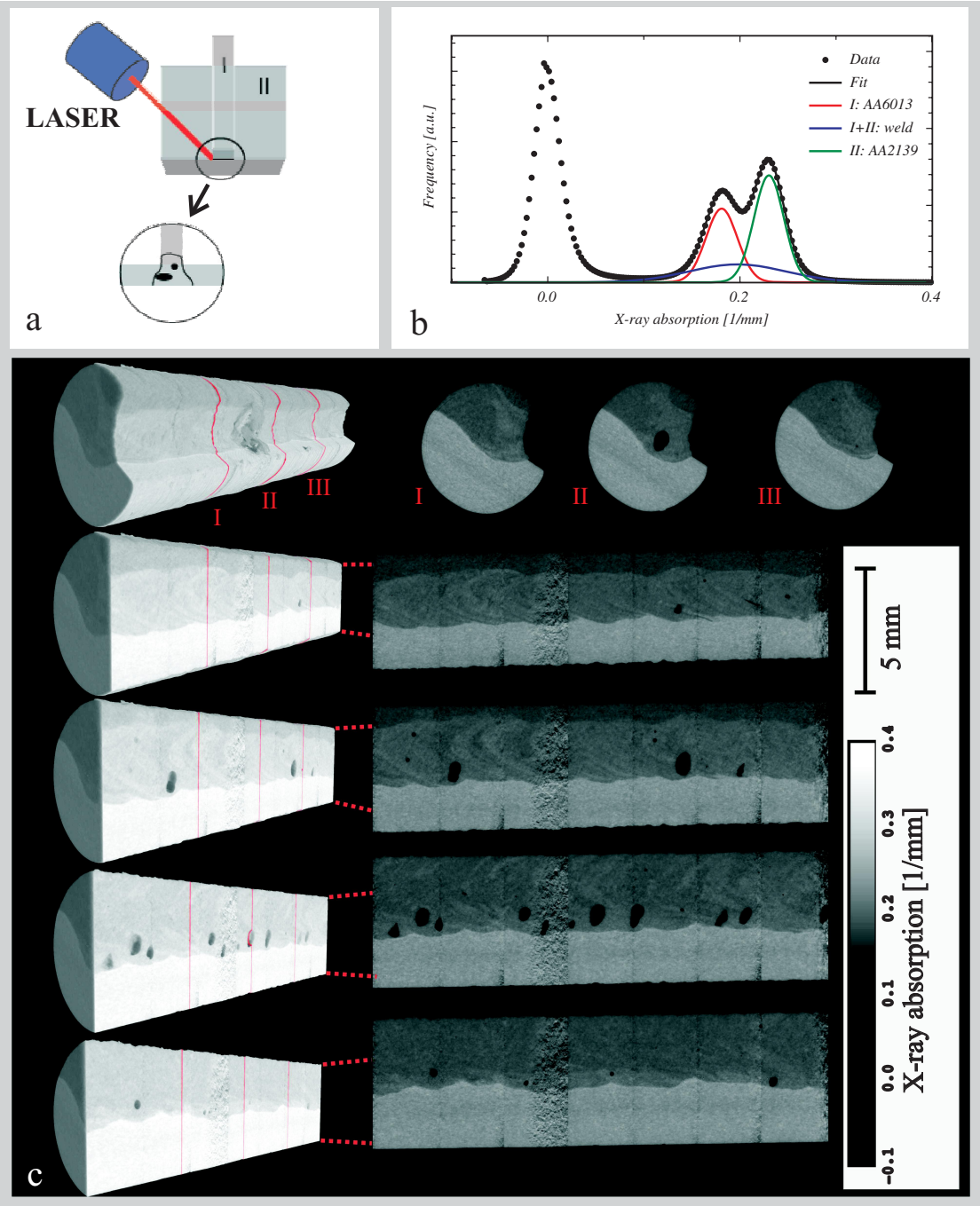

Figure 5. Microtomography study using 40 keV photon energy at beamline W2/HARWI-II. Several scans were recorded to investigate a significant part of the specimen. a: Scheme of the laser welding process. The laser-welded clip consists of two aluminum alloys (I: AA6013 T6, II: AA2139 T3). The cylindrical sample 30 mm long and 6 mm in diameter was prepared cutting from the weld region (as marked by the inset). b: Histogram of the total reconstructed volume revealing the different materials. The aluminum peaks can be fitted with three Gaussian representing the two alloys and the weld region. c: Volume renderings of the tomogram and several virtual cuts. The corresponding slices are given revealing the differently absorbing materials and various sizes of pores in the weld.

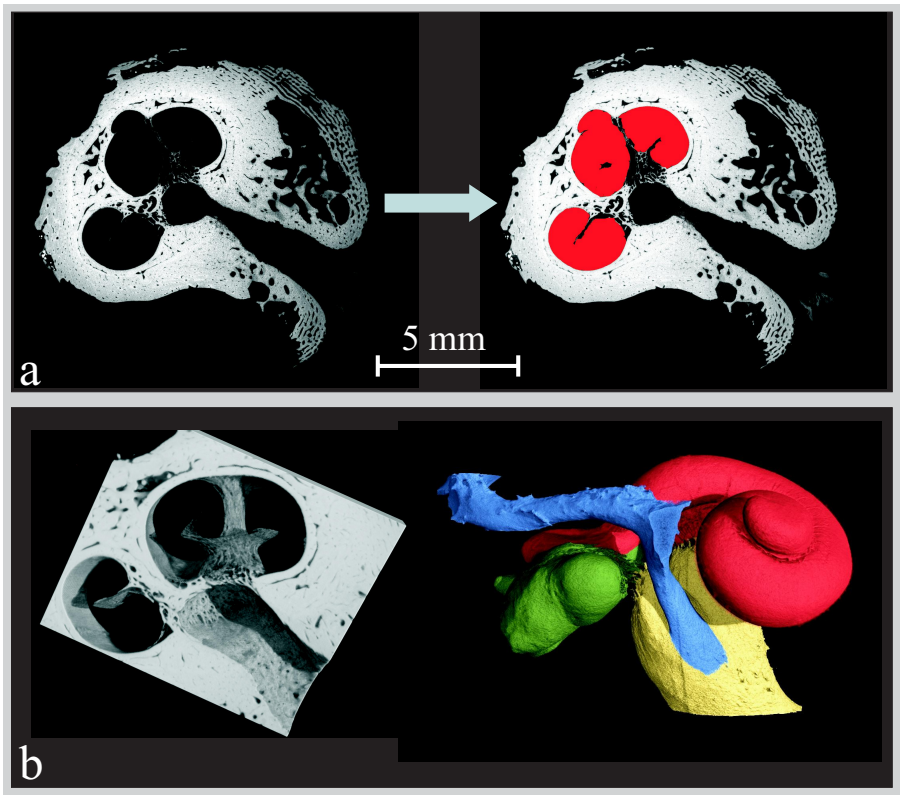

Figure 6. SRμCT study of the vestibular and cochlear labyrinth of a patient diagnosed with CHARGE syndrome. The temporal bone specimen was investigated by applying scanning techniques using the photon energy of 40 keV at the beamline W2/HARWI-II. The total reconstructed volume is 16.2 x 16.2 x 24.5 mm^3. a: The virtual slice through the reconstructed volume reveals the liquid filled labyrinth. On the right, the cochlear labyrinth is segmented and colored in red. b: On the left, the volume rendering shows the bony structures in the cochlear and on the right, the vestibular labyrinth is visualized in green, the cochlear labyrinth in red, and different nerves in blue and yellow.

4. RESULTS

To demonstrate the high spatial and density resolution of the present tomography system using synchrotron radiation at DORIS III, DESY, a few typical examples representing the different research areas are selected.

4.1 Materials Science

In materials science SRμCT has evolved as an increasingly utilized technique for the characterization of the 3D microstructure of materials.[5] At the GKSS Research Center Geesthacht new materials and joining techniques are developed and characterized using SRμCT at DESY.[17,18]

Laser-welded aluminum T-Joints

Here we present a study for the 3D characterization of laser-welded aluminum alloy T-joints. The sample preparation is shown in figure 5a. A more precise description of the welding process and sample preparation is given in this proceedings.[19] The total reconstructed volume of the shown sample consists of 1536 x 1536 x 4180 voxels representing a volume of 7.0 x 7.0 x 19.0 mm^3. Several tomographical scans were performed at different heights of the sample using a phonon energy of 40 keV at beamine W2/HARWI-II. The attenuation values histogram of the total volume is given in figure 5b. The high photon statistics allows for the separation of several materials. The Al-peak can be fitted with three Gaussians to allow distinguishing the different Al-alloys and the welding region. In figure 5c volume renderings with related virtual cuts and the corresponding calculated slices are shown. The different components can be clearly identified and pores sizes in the weld can be evaluated.

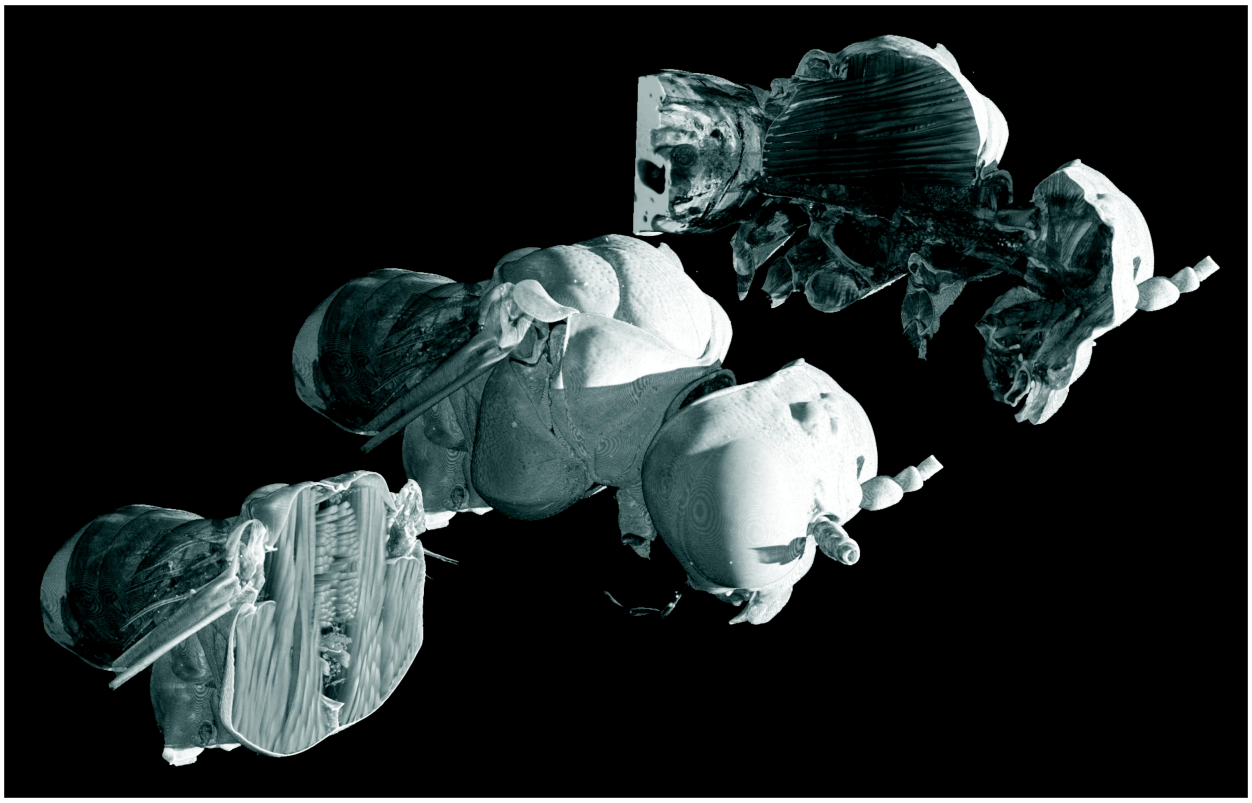

Figure 7. Volume renderings of the head and thorax of the sawfly Tenthredo vespa. The SRμCT was performed at beamline BW2 of DORIS III using a photon energy of 8 keV. Due to the large and incoherent source, pure absorption-contrast was applied at low photon energies to visualize the different parts of the external and internal anatomy of the sawfly, e.g. the different types of muscles, antenna, eyes. (length of the specimen 7.3 mm).

4.2 Inner ear research

SRμCT techniques are widely used in medical applications. The 3D morphology of bony tissues and implants are nowadays routinely studied.[14] The characterization of bone replacement materials with the demand to reveal the ingrowth of cells becomes only possible by using high density resolution SRμCT.[20] Here we present a morphological study in a patients diagnosed with CHARGE* syndrome. We evaluated the histopathological changes of the vestibular and cochlear labyrinth. The temporal bone was studied using SRμCT using 40 keV photon energy at beamline W2/HARWI-II. As the sample was larger than the field of view of the detector the rotation axis was shifted to the side of the field of view. The tomographical scan was increased to cover 2π rotation. Before reconstruction projections shifted by π were combined to build one projection. Furthermore, the scans were recorded for several heights of the sample resulting in a reconstructed volume of 1502 x 1509 x 2277 voxels representing 16.2 x 16.2 x 24.5 mm^3. The high quality of the SRμCT data allows yielding information about the 3D gross morphology including visualization of the bony and membranous labyrinth structures. Particular interest was directed to the preservation of sensory structures within the organ of Corti and innervation pattern. The vestibular partition consisted of a rudimentary vestibulum with agenesis of the semicircular canals. In figure 6 virtual cuts through the volume, the registration and visualization of the liquid filled vestibular and cochlear labyrinth are shown.

4.3 Zoology

The application of SRμCT in zoological science becomes more and more important. The technique allows for a direct representation of the 3D structures and is used to accompany and/or replace standard histological

*C: Coloboma, H: Heart defect, A: choanalAtresia, R: Retardation, G: Genital hypolasia, E: Ear anomalies

techniques to obtain morphological data for the understanding of body structures of animals.[21–23] Recently X-ray phase contrast techniques have been developed, but only the phase-outline contrast SRμCT method is applied in user mode at third generation synchrotron radiation facilities. The interfaces are highlighted in the tomogram. Pure phase contrast methods, which maps the phase shift in the projections, require more effort and are, therefore, not yet available as standard user technique. For samples consisting mainly of low absorbing elements, using the optimum photon energy for absorption contrast at the high flux synchrotron radiation source DORIS III at DESY allows for a user experiment resulting in high density resolution tomograms.[24,25] In figure 7 volume renderings of the head and thorax of the sawfly Tenthredo vespa are shown for selected virtual cuts. The SRμCT was performed at beamline BW2 using the photon energy of 8 keV. The specimen was scanned at three heigths resulting in a total reconstructed volume of 1536 x 1536 x 2196 voxels representing 6.0 x 6.0 x 8.6 mm^3. Due to the large and incoherent source, pure absorption-contrast showing a high density resolution was applied at low photon energies to distinguish the parts of the external and internal anatomy of the sawfly, including muscles, antenna, eyes.[25]

5. SUMMARY AND OUTLOOK

It is demonstrated that SRμCT at the incoherent synchrotron radiation source DORIS-III at DESY is the ability to perform pure absorption-contrast microtomography showing not only high spatial resolution but also high density resolution. To compete with the currently available μCT at conventional X-ray sources the focus on the artefact-free mapping of the attenuation is important. To further increase the density resolution and the spatial resolution in the tomograms of large objects a dedicated microtomography apparatus for beamline W2/HARWI-II is under construction and will become available mid of 2009. By using 16bit CCD systems and air-bearing nano manipulators, including an automatic sample changer, the throughput of the system will be increased at enhanced spatial and density resolution in the tomograms.

In combination with the availability of the beamlines for imaging at the third generation storage ring PETRA III the combination of coarse tomography at DORIS III with the advanced micro- and nanotomography at PETRA III will provide for complete tomographic investigation tools covering wide spectrum of applications in biology, medicine, and materials science.

ACKNOWLEDGMENTS

Thank is due to A. Schrott-Fischer, R. Glueckert and J. Schmutzhart Innsbruck Medical University, Austria, for providing the temporal bone sample. For the fruitful discussion and for the shown insect data we thank F. Friedrich, M. Nickel, and R.G. Beutel, Friedrich-Schiller-University Jena, Germany. S. Riekehr, F.S. Bayraktar, M. Kocak, GKSS, we thank for the cooperation in the laser weld project. For the operation of the beamlines at DORIS III thank is due to the HASYLAB staff and the GKSS staff at the beamlines.

REFERENCES

[1] Beckmann, F., Donath, T., Dose, T., Lippmann, T., Martins, R., Metge, J., and Schreyer, A., "Microtomography using synchrotron radiation at DESY: current status and future developments," *SPIE Proceedings* **5535**, 1–10 (2004).

[2] Germann, M., Morel, A., Beckmann, F., Andornache, A., Jeanmonod, D., and Müller, "Strain fields in histological slices of brain tissue determined by synchrotron radiation-based micro-computed tomography," *Journal of Neuroscience Methods* **170**, 149–155 (2008).

[3] Schurigt, U., Hummel, K., Petrow, P., Gajda, M., Stöckigt, R., Middel, P., Zwerina, J., Janik, T., Bernhardt, R., Schüler, S., Scharnweber, D., Beckmann, F., Saftig, P., Kollias, G., Schett, G., Wiederanders, B., and Bräuer, R., "Cathepsin K Deficiency Partially Inhibits, But Does Not Prevent, Bone Destruction in Human Tumor Necrosis FactorTransgenic Mice," *Arthritis & Rheumatism* **58**(2) (2008).

[4] Beckmann, F., Donath, T., Fischer, J., Dose, T., Lippmann, T., Lottermoser, L., Martins, R., and Schreyer, A., "New developments for synchroton-radiation based microtomography at DESY," *Proc. of SPIE* **6318**, 631810 (2006).

[5] Beckmann, F., Dose, T., Lippmann, T., Martins, R., and Schreyer, A., "The New Materials Science Beamline HARWI-II at DESY," *AIP Conference Proceedings, SRI2006, Daegu, Korea* **CP879**, 746–749 (2007).

[6] Haibel, A., Beckmann, F., Dose, T., Herzen, J., Utcke, S., Lippmann, T., Schell, N., and Schreyer, A., "The GKSS Beamlines at PETRA III and DORIS III," *Proc. of SPIE* **7078** (2008).

[7] Beckmann, F., "Neutron and synchrotron-radiation based imaging for applications in materials science from macro- to nanotomography," *In Reimers, W., Pyzalla, A.R., Schreyer, A. and Clemens, H., [Neutrons and synchrotron radiation in engineering materials science], Wiley-VCH, Weinheim* , 287–370 (2008).

[8] Drube, W., Schulte-Schrepping, H., Schmidt, H.-G., Treusch, R., and Materlik, G., "Design and performance of the high-flux/high-brightness x-ray wiggler beamline BW2 at HASYLAB," *Rev. Sci. Instrum.* **66**, 1668–1670 (1995).

[9] Schulte-Schrepping, H., Heuer, J., and Hukelmann, B., "Adaptive indirectly cooled monochromator crystals at HASYLAB," *J. Synchrotron Rad.* **5**, 682–684 (1998).

[10] Huesman, R. H., Gullberg, G. T., Greenberg, W. L., and Budinger, T. F., [*Reclbl Library Users Manual*] (1977).

[11] Donath, T., Beckmann, F., and Schreyer, A., "Automated determination of the center of rotation in tomography data," *J. Opt. Soc. Am. A* **23**(5), 1048–1057 (2006).

[12] Grodzins, L., "Optimum energies for x-ray transmission tomography of small samples," *Nucl. Instrum. Methods* **206**, 541545 (1983).

[13] Schneiders, N. J. and Bushong, S. C., "Single-step calculation of the MTF from the ERF," *Med. Phys.* **5**(1), 31–33 (1978).

[14] Müller, B., Bernhardt, R., Weitkamp, T., Beckmann, F., Bräuer, R., Schurigt, U., Schrott-Fischer, A., Gluecker, R., Ney, M., Beleites, T., Jolly, C., and Scharnweber, D., "Morphology of bony tissues and implants uncovered by high-resolution tomographic imaging," *Int. J. Mat. Res. (formerly Z. Matallkd.)* **98**(7) (2007).

[15] Beckmann, F. and Bonse, U., "Attenuation and phase-contrast microtomography using synchrotron radiation for the 3-dim. investigation of specimens consisting of weakly and normally absorbing elements," in [*Applications of Synchrotron Radiation Techniques to Material Science V*], Stuart R. Stock, Susan M. Mini, D. L. P., ed., *Mat. Res. Soc. Symp. Proc.* **590**, 265–271 (2000).

[16] Thurner, P., Beckmann, F., and Müller, B., "An optimization procedure for spatial and density resolution in hard x-ray micro-computed tomography," *Nucl. Instr. and Meth. in Phys. Res. B* **225**, 599–603 (2004).

[17] Zettler, R., Donath, T., dos Santos, J., Beckmann, F., and Lohwasser, D., "Validation of Marker Material Flow in 4mm Thick Friction Stir Welded Al 2024-T351 through Computer Microtomography and dedicated Metallographic," *Adv. Eng. Mater.* **8**, 487–621 (2006).

[18] Amancio-Filho, S., Roeder, J., Nunes, S., dos Santos, J., and Beckmann, F., "Thermal degradation of polyetherimide joined by friction riveting (FricRiveting). Part I: Influence of rotation speed," *Polymer Degradation and Stability* **in Press** (2008).

[19] Herzen, J., Beckmann, F., Riekehr, S., Bayraktar, F., Haibel, A., Staron, P., Donath, T., Utcke, S., Kocak, M., and Schreyer, A., "SRμCT study of crack propagation within laser-welded aluminum-alloy T-joints," *Proc. of SPIE* **7078** (2008).

[20] Fierz, F., Beckmann, F., Huser, M., Irsen, S., Leukers, B., Witte, F., Degistirici, O., Andronache, A., Thie, M., and Müller, B., "The morphology of anisotropic 3d-printed hydroxyapatite scaffolds," *Biomaterials* **29**, 3799–3806 (2008).

[21] Kleinteich, T., Beckmann, F., Herzen, J., Summers, A., and Haas, A., "Applying X-ray tomography in the field of vertebrate biology: form, function, and evolution of the skull of caecilians (Lissamphibia: Gymnophiona)," *Proc. of SPIE* **7078** (2008).

[22] Nickel, M., Bullinger, E., and Beckmann, F., "Functional morphology of Tethya species (Porifera): 2. three-dimensional morphometrics on spicules and skeleton superstructures of T. minuta," *Zoomorphology* **125**, 225–239 (2006).

[23] Nickel, M., Donath, T., Schweikert, M., Bullinger, E., and Beckmann, F., "Functional morphology of Tethya species (Porifera): 1. quantitative 3D-analysis of T. wilhelma by synchrotron radiation based x-ray microtomography," *Zoomorphology* **125**, 209–223 (2006).

[24] Nickel, M., Hammel, J., Herzen, J., Bullinger, E., and Beckmann, F., "High Density Resolution Synchrotron Radiation based X-Ray Microtomography (SRμCT) for quantitative 3D-Morphometrics in Zoological Sciences," *Proc. of SPIE* **7078** (2008).

[25] Friedrich, F. and Beutel, R., "Micro-computer tomography and a renaissance of insect morphology," *Proc. of SPIE* **7078** (2008).